# Self-consistent pseudopotential calculation of electronic states associated with a reconstructed silicon vacancy

M. Jaros, C. O. Rodriguez, and S. Brand
*Department of Theoretical Physics, The University Newcastle upon Tyne, United Kingdom*
(Received 22 August 1978)

We have extended our pseudopotential method and carried out a self-consistent calculation of electronic states associated with a single vacancy in silicon, with a particular emphasis on the problem of lattice reconstruction in the vicinity of the defect. We find that the vacancy with three dangling electrons, i.e., $V_{Si}^{+}$, has a localized state close to the valence-band edge. We show that the nonspherical part of the vacancy potential, which is related to the rearrangement of the electron charge density along the bonding directions, plays an important part in the quantitative assessment of the position of the bound state in the gap. The lattice reconstruction consists of a symmetric, outward displacement of the nearest-neighbor silicon atoms by about 0.1 Å, and a similar tetragonal displacement that gives rise to a characteristic splitting of the degenerate $t_2$ state in the gap. The final lattice configuration is deduced from minimum-energy considerations. The net reduction in the total energy associated with the lattice reconstruction is about 1 eV. A critical discussion of the results is given in the light of existing theoretical and experimental evidence.

## I. INTRODUCTION

There are several ways in which the regularity of a perfect lattice may be destroyed. If we, for instance, remove a host atom and replace it with a foreign one, we can model such an event by writing the total Hamiltonian as $H_0 + V$, where $H_0$ represents the perfect-crystal part and $V$ is the contribution of the defect. In the limit $V \to 1/\epsilon_0 r$, the effect of $H_0$ is to engage primarily contributions from a small fraction of the Brillouin zone near the principal band minima and the solution of the Schrödinger equation resembles that of a hydrogen atom immersed in a dielectric medium.[1] However, in the presence of a strong, short-range potential $V$, the Schrödinger equation must be solved numerically. The dominant role of the short-range forces in the formation of localized states cannot be modeled by assuming that the properties of the defect are determined by those of the free atom, with the effect of lattice environment taking part only as a perturbation. Calculations based on cluster schemes show that in covalent crystals like silicon it is not sufficient to describe the characteristics of the defect by surrounding it with a few nearest-neighbor atoms in the lattice.[2-4] It has become apparent that the effects of $H_0$ and $V$ should be treated on an equal footing. Just as the success of the hydrogenic model lies in a skillful exploitation of the long-range character of $V$, the theory of localized ("deep") states must benefit in full from the short-range nature of $V$, and the present knowledge of the band structure of perfect crystals. Recently, we have performed pseudopotential calculations which demonstrate that *given* $H_0$ *and* $V$, *a convergent solution* of the Schrödinger equation can be obtained.[5,6] Our findings compare favorably with subsequent calculations carried out by other authors in a similar spirit.[7,8] The short-range interactions also affect the electron distribution in the vicinity of the defect and a *self-consistent* calculation of the total charge density, allowing for lattice *relaxation*, must be performed. From a change in the total energy of the system, the most energetically favorable configuration can be found. This part of the calculation is much less understood, although some insight has been provided by Louie *et al.*[9] These workers computed the electronic structure of a vacancy in Si within the self-consistent-pseudopotential approach, using a large-unit-cell model. Although the method of Louie *et al.* does not allow for a very accurate determination of the position of bound states in the gap, it does show that the *average* vacancy potential is not very different from that of a neutral pseudoatom extracted from band-structure calculations.

The vacancy problem in Si is an ideal one to study because it is relatively well understood experimentally. In a series of elegant ESR experiments, Watkins and Elkins and Watkins[10-14] have shown that a vacancy in Si has at least three different charge states, $V_{Si}^{+}$, $V_{Si}^{0}$, and $V_{Si}^{-}$, with levels in the gap separated by about 0.2 eV. The nearest-neighbor silicon atoms relax from their perfect-lattice positions and the spectra indicate an angular displacement of ~7° from the perfect ⟨111⟩ to ⟨100⟩ directions. The stress dependence of the ESR signal points to a Jahn-Teller splitting. The bound state associated with $V_{Si}^{+}$ appears to be lying very close to the top of the valence band.[14,15]

In this paper we present a study of the vacancy in silicon, with particular emphasis on the problem of lattice distortion. We have extended our

 

pseudopotential scheme and carried out a self-consistent calculation of the electronic states in the reconstructed silicon lattice. We compute the changes in the total energy of the system in order to assess the minimum-energy configuration.

In Sec. II we outline our approach. We define our objectives in quantitative terms and argue that it may be advantageous to divide the problem into several parts and tailor the methods of dealing with them separately. In Sec. III, we present the results of our calculation concerning a positively charged vacancy in silicon. In Sec. IV, a critical assessment of the results is given, and the paper is concluded with a brief summary.

## II. SELF-CONSISTENT DEFECT CALCULATIONS IN A RECONSTRUCTED LATTICE

The problem of solving a Schrödinger equation, $(H_0+V)\Psi=\epsilon\Psi$, with a strong short-range potential $V$, can be divided into three parts. (i) The band structure of the host crystal is generated and a trial potential $V$ chosen. The bound states in the gap are then computed. (ii) The total energy and charge density in the presence of $V$ are calculated. (iii) The potential $V$ is readjusted and the calculation repeated until a self-consistent result is obtained. The reconstruction of the lattice is then allowed for and the process is reiterated until a minimum-energy configuration is found.

### A. Localized states

It has been shown how to solve the Schrödinger equation, given the perfect-crystal band structure and a localized potential $V$. The details of the method of calculation have been published[5,6] and will not be described here. We begin with the one-electron Schrödinger equation,

$$H\Psi=\epsilon\Psi\,, \tag{2.1}$$

where $H$ is split into two terms,

$$H=H_0+V\,. \tag{2.2}$$

Here $H_0$ represents the perfect-crystal Hamiltonian and $V$ stands for the extra potential introduced by the imperfection and its environment. The wave function $\Psi$ is represented in terms of an expansion in the complete set of host-crystal eigenfunctions $\Phi_{n,\vec{k}}$

$$\Psi=\sum_n \int_{BZ} A_{n,\vec{k}}\Phi_{n,\vec{k}}\,d\vec{k} \tag{2.3}$$

where the integration extends over the volume of the first Brillouin zone; $n$ indicates summation over all bands. Inserting the expansion of (2.3) in (2.1), multiplying from the left by $\Phi^*_{n',\vec{k}'}$, and integrating we obtain a set of linear equations,

$$A_{n',\vec{k}'}(E_{n',\vec{k}'}-\epsilon)+\sum_n \int_{BZ} d\vec{k}A_{n,\vec{k}}\int d\vec{r}\,\Phi^*_{n',\vec{k}'}(\vec{r})V\Phi_{n,\vec{k}}(\vec{r})=0\,, \tag{2.4}$$

where $E_{n',\vec{k}'}$ represents the relevant energy associated with a reduced wave vector $\vec{k}'$ and band $n'$ such that

$$H_0\Phi_{n',\vec{k}'}=E_{n',\vec{k}'}\Phi_{n',\vec{k}'}\,. \tag{2.5}$$

A complete set of localized functions $g$ is employed so as to rewrite the matrix elements in (2.4).[16] Since for such a set we can write

$$\int d\vec{r}'\,\delta(\vec{r}-\vec{r}')=\sum_m \int d\vec{r}'\,g^*_m(\vec{r}')g_m(\vec{r})\,, \tag{2.6}$$

Eq. (2.4) is replaced by

$$A_{n',\vec{k}'}(E_{n',\vec{k}'}-\epsilon)+\sum_m\sum_n \int d\vec{k}A_{n,\vec{k}}f^*_m(n',\vec{k}')f_m(n,\vec{k})=0\,, \tag{2.7}$$

where

$$f_m(n,\vec{k})=\int d\vec{r}\,g^*_m(\vec{r})V^{1/2}(\vec{r})\Phi_{n,\vec{k}}(\vec{r})\,. \tag{2.8}$$

The impurity potential $V$ enters in a factorized form, i.e., as a product $V^{1/2}V^{1/2}$ or, more generally,

$$V=V_iV_j\,. \tag{2.9}$$

For a multicenter defect several sets of functions may have to be used. Let us now define

$$a_m=\sum_n \int_{BZ} d\vec{k}A_{n,\vec{k}}f_m(n,\vec{k}) \tag{2.10}$$

so that Eq. (2.7) becomes

$$A_{n',\vec{k}'}(E_{n',\vec{k}'}-\epsilon)+\sum_m a_mf^*_m(n',\vec{k}')=0\,. \tag{2.11}$$

If we look for states with energies $\epsilon$ in the forbidden gap of the host crystal, i.e.,

$$E_{n',\vec{k}'}-\epsilon\neq 0 \tag{2.12}$$

we can divide (2.11) by $E_{n',\vec{k}'}-\epsilon$, multiply by $f_m(n',\vec{k}')$, and sum over all $n',\vec{k}'$ to obtain a new set of equations for the $a_m$'s:

$$a_{m'}+\sum_m a_m\sum_n \int_{BZ} d\vec{k}\frac{f^*_m(n,\vec{k})f_m(n,\vec{k})}{E_{n,\vec{k}}-\epsilon}=0\,. \tag{2.13}$$

The bound states must occur at energies $\epsilon$ such that

$$\det\left| \delta_{m',m} + \sum_n \int_{BZ} d\vec{k} \frac{f_m^*(n,\vec{k}) f_{m'}(n,\vec{k})}{E_{n,\vec{k}} - \epsilon} \right| = 0 . \quad (2.14)$$

The wave function $\Psi$ in the wave-vector space is determined via the expansion coefficients of Eq. (2.13) which are related to $a_m$, $\epsilon_i$:

$$A_{n,\vec{k}} = \sum_m a_m \frac{f_m^*(m,\vec{k})}{\epsilon_i - E_{n,\vec{k}}} . \quad (2.15)$$

The wave function at a particular point $\vec{r}_j$ in real space is generated numerically by computing

$$\Psi(\vec{r}_j) = \sum_n \int_{BZ} d\vec{k} A_{n,\vec{k}} \Phi_{n,\vec{k}}(\vec{r}_j) . \quad (2.16)$$

Symmetry considerations greatly reduce the amount of computation.

It has been shown that typically ten bands and 41 $\times 48$ general points in the first Brillouin zone constitute an adequate sample to produce a convergent solution. About ten functions $g$ are required. They were chosen to be represented by products of the associated Laguerre polynomials and spherical harmonics. The convergence in g's is optimized by varying the range of the polynomials according to the range of the potential $V$.[17]

As the Eqs. (2.13) and (2.14) indicate, the Green's-function formulation does not remove the sums over the wave-vector space. Indeed, each element in (2.14) contains such a sum, i.e., the sum over all sampling points and all bands. As a computational exercise, these sums can be evaluated in seconds and because $g$'s are basically polynomials, the sums are in fact evaluated only once for each power of $r$ and each angular momentum component. This formulation greatly simplifies the convergence procedure in comparison with the requirements normally present in techniques similar in spirit (e.g., Koster-Slater[18] method). In the presence of a strong potential $V$, the integrals $f_m(n,\vec{k})$ are large numbers. Also the sum $\sum_{BZ} 1/(E_{n,\vec{k}} - \epsilon)$ is very slow to converge.[19,20] Fortunately, the terms under the sum in (2.14) must, to a large degree, cancel as we add contributions from valence and conduction bands, and from various sampling points, reflecting different symmetry relationships between the localized functions and the Bloch states.

The large number of bands required shows quite clearly that the "binding energy" $\epsilon$, normally defined with respect to the nearest band edge, is a result of cancellations of terms much larger than $\epsilon$. The composition of the wave function $\Psi$ also exhibits this trend.[5,21] It follows that the localization of the wave function is *not* necessarily a sensitive function of the actual magnitude of $\epsilon$, since the localization cannot be thought of in terms of the magnitude of $\epsilon$ only. Indeed, the wave function is made up of a large number of coefficients $A_{n,\vec{k}}$, coming from an area of a width of ~30 eV.[5]

Let us suppose that we wish to solve (2.1), allowing for lattice reconstruction. It means that $V$ becomes a multicenter term and the length and complexities involved in executing the above equations increase dramatically. These difficulties are amplified even further by self-consistency requirements which introduce more angular structure into the potential and demand that the whole calculation be repeated many times. Much of the complexity is closely related to the choice of the functions $g$ and it may well be that functions of a more sophisticated form would give an improvement. However, the *completeness* requirement is an important one and makes a suitable mathematically *rigorous* substitute for our $g$'s difficult to find. It means that more or less plausible approximations would have to be made at this stage, by choosing a new set of functions $g$ in a semiempirical way, and restructuring the procedure accordingly.

It is borne in mind that the *overall strength* of the corrections to $V$ due to self-consistency and lattice distortion, $\delta V$, must be typically small compared to $V$. Since it has been shown[21] that changes in the binding energy measured from the band edge, caused by a small adjustment of the potential $V$, do not drastically alter the form of the wave function $\Psi$, such a proposition is an attractive one. For one can simply take the dominant, one- or two-center part of $V$ and solve the Schrödinger equation with great accuracy following the established procedure [Eqs. (2.1) and (2.14)]. Having found $\epsilon$ and a set of $A_{n,\vec{k}}$'s associated with a particular bound state, we can complete the calculation following a different, much *simpler* and still quite rigorous procedure.[21]

The Schrödinger equation

$$(H_0 + V)\Psi = \epsilon\Psi \quad (2.17)$$

can also be written as

$$\left(H_0 + \frac{V|\Psi'\rangle\langle\Psi'|}{\langle\Psi'|V|\Psi'\rangle}\right)\Psi = \epsilon\Psi . \quad (2.18)$$

Expanding $\Psi$ in Bloch states (2.3) leads to

$$1 + \frac{1}{\langle\Psi'|V|\Psi'\rangle} \sum_{n,\vec{k}} \frac{|\langle\Phi_{n,\vec{k}}|V|\Psi'\rangle|^2}{E_{n,\vec{k}} - \epsilon} = 0 , \quad (2.19)$$

which is automatically satisfied if $\Psi' \to \Psi$. Having established $\Psi$ and $\epsilon$, we can seek $\epsilon + \delta\epsilon$ associated with $V + \delta V$ by repeating (2.18) until after the $n$th iteration $\Psi^n \approx \Psi^{n-1}$ and $\epsilon^n \approx \epsilon^{n-1}$. The procedure in (2.18) is so easy to execute that practically any number of iterations with any $\delta V$ are possible.

### B. Self-consistent potentials

In the absence of translational symmetry, the methods normally used to generate self-consistent pseudopotentials do not apply and the problem of finding a satisfactory solution may be a difficult one. For periodic systems, dielectric screening (i.e., perturbation theory) has been quite a successful substitute for exacting and more laborious procedures. The pseudopotential representation of potentials for atoms in perfect lattices are smooth and weak, and they add together in such a way that the final crystal potential is rather flat.[22,23] Also, the relevant contributions participating in the screening process for such a system are the Fourier components of the potential at the first few reciprocal-lattice vectors only. In particular, the large components near $\vec{k} \approx 0$ are not needed. In the vicinity of a defect, the perfect crystalline symmetry is broken and matrix elements of the impurity potential $V$ are in principle finite at any point in the wave-vector space. All those terms then enter the screening formalism. If $V$ is strong and of short range, the total potentials change abruptly and the perturbation formalism might be expected to break down. The electron screening potential is related to a change in the valence charge density $\delta\rho$ which is proportional to[23]

$$\sum_{n',\vec{k}'} \sum_{n'',\vec{k}''} \frac{\langle \Phi_{n',\vec{k}'} | V | \Phi_{n'',\vec{k}''} \rangle}{E_{n'',\vec{k}''} - E_{n',\vec{k}'}} \Phi_{n'',\vec{k}''} \Phi_{n',\vec{k}'} + \text{c.c.} \tag{2.20}$$

In the notation of Eqs. (2.1) and (2.13), we would write this as

$$\sum_{n',\vec{k}'} \sum_{n'',\vec{k}''} \left( \sum_m f_m^*(n',\vec{k}') f_m(n'',\vec{k}'') \right) \Big/ (E_{n'',\vec{k}''} - E_{n',\vec{k}'}) \Phi_{n'',\vec{k}''} \Phi_{n',\vec{k}'} + \text{c.c.} \tag{2.21}$$

Here $n',\vec{k}'$ and $n'',\vec{k}''$ refer to occupied and unoccupied states, respectively. If we decided to use the Green's-function technique to compute the change in the valence-electron charge density, the leading term directly comparable to those in (2.20) and (2.21) becomes

$$\sum_{n',k'} \sum_{n'',k''} \left[ \sum_m f_m(n'',\vec{k}'') \left( f_m^*(n',\vec{k}') + \sum_{n,\vec{k}} A_{n,\vec{k}} f_m(n,\vec{k}) \right) \right] \Big/ (E_{n'',\vec{k}''} - E_{n',\vec{k}'}) \Phi_{n'',\vec{k}''} \Phi_{n',\vec{k}'} . \tag{2.22}$$

It is apparent that although each contribution in the sum over $n,\vec{k}$ may be large because of the strength of $V$, the sum should reflect the cancellations familiar from our observation in the above paragraphs, and the final result should not be too different from that given by the approximate expressions in (2.20) and (2.21).

The wave-vector-dependent dielectric function $\epsilon(\vec{q})$ has been studied extensively.[24-26] In spite of these efforts, $\epsilon$ is probably not known with more than 10%–15% accuracy. It is doubtful that we could aim at obtaining charge densities in imperfect systems with much greater precision. Even if much of the calculation can be done in the wave-vector space, the results must be processed at several stages and an additional error is inevitable. It is with these considerations in mind that we must approach any assessment of numerical calculations involving the charge density in the presence of a localized potential.

The most detailed study of self-consistency was performed by Louie *et al.*[9] who employed a large unit cell of 54 atoms to compute the silicon vacancy potential. The *average* potential associated with a neutral vacancy in the unrelaxed lattice came out very similar to that of a neutral pseudoatom. The changes in the charge density outside the nearest-neighbor distance were small. This suggests that a similar result could be obtained with much simpler means. In Fig. 1, we compare the potential of Louie *et al.* with that obtained from our calculation in which every primitive cell of Si contains one vacancy. Since the procedure for generating the potential was exactly the same in both cases, the comparison may be taken to indicate that at least the dominant contribution to the change in the charge density comes from within the Wigner-Seitz cell of the defect.

The calculation of the electron charge density requires that a sum of all changes in the valence band be evaluated. The localized potential can give rise to states degenerate with the solutions of the perfect-crystal Hamiltonian. These resonances must also be taken into account since their contribution to the total charge density might be significant. On the other hand, a precise position of such a resonance in the band is not really important.

The solutions of the Schrödinger equation at the sampling points which span the width of the valence band should also yield a change in energies of all occupied states included in the sample. Hence the problem of self-consistency is inseparable from the problems associated with calculations of the lattice distortion and total energy.

### C. Total energy of a system containing a defect in a reconstructed lattice

In a reconstructed lattice, the defect potential becomes a complicated function of a multicenter character.[9,27-29] The practical considerations must take into account this fact, since we would pay a high price for relying on symmetry to simplify our computations; in some cases, we must study displacements which leave us with an "amorphous" block of the material to deal with. Since we have independent means of solving the Schrödinger equation for *bound states*, and since only a few points in the Brillouin zone seem sufficient to carry out the sums over the occupied states in the valence band[9,27-29] the most attractive proposition is to turn to the direct-matrix problem in Eq. (2.4). It is very convenient to be able to set up the matrix elements of the potential $V$ in the wave vector space, where the multicenter character of $V$ presents no difficulties.[30] With thirty points in the Brillouin zone and including the eight lowest bands, the computer returns $30\times 8$ eigenstates which are linear combinations of $30\times 8$ unperturbed eigenfunctions. The integrals over the valence band are then constructed from these data, giving the electronic charge density and the band-structure contribution to the total energy, i.e., $2\sum E_i(\mathrm{occ})$. Since in summing over all occupied states we count the electron-electron interaction twice, we must subtract $\int V_{el}\rho\, d\tau$ once in the expression for the total energy. The procedure of carrying out a self-consistent pseudopotential calculation of charge densities is formally the same as that for the large-unit-cell scheme of Louie *et al.*[9] From a practical point of view, our scheme is much simpler to execute and a very general one, so that a defect complex of *any* zinc-blende lattice can be studied with only minor modifications of the computer program. Although the *localized states* in the gap are also returned in the calculations, their position on an absolute scale must be subject to an error due to the dispersion of the kind discussed earlier.[9] However, the *relative* changes, i.e., splittings and shifts due to small alterations in the potential may be well represented. As pointed out earlier,[21] the localized wave functions do not change as significantly in such a process as one might expect in the spirit of the effective-mass theory.

The changes in the energy of the individual "sampling" states in the *valence band*, due to the presence of a localized potential $V$, are typically of the order of 1% or less for the sample of 30 points, and should give a good representation of the change in the electron energy. It should be understood that here we are really interested in the change in the total energy of the system associated with the presence of a defect, e.g., a vacancy, i.e.,

$$\delta E_T = 2\sum \delta E_{\mathrm{occ}} - \int V_e \delta\rho\, d\tau + \delta E_{ii}\,, \qquad (2.23)$$

where $\delta E_{\mathrm{occ}}$, $\delta\rho$ refer to the changes in one-electron energies and charge densities and $V_e$ is the potential related to the electron rearrangement. The sum is over all occcupied states. $\delta E_{ii}$ is the energy of the bare ions.

In order to evaluate $\delta E_T$, we require the potential $V$ at the sites of the displaced ions in the reconstructed lattice. From Fig. 1 we can see that at about the nearest-neighbor distance, the potential is a small fraction of its value at the maximum. The problem of finding a meaningful estimate of $V$ far from the defect is a formidable one since the calculation at the long-wavelength limit is strongly model dependent. Furthermore, the charge density and the "bare" pseudopotential must be converted from the wave-vector space into the real one, hence enforcing an additional error. The question of representing long-range forces has been discussed at some length in a similar context.[22,28,29] The magnitude of the po-

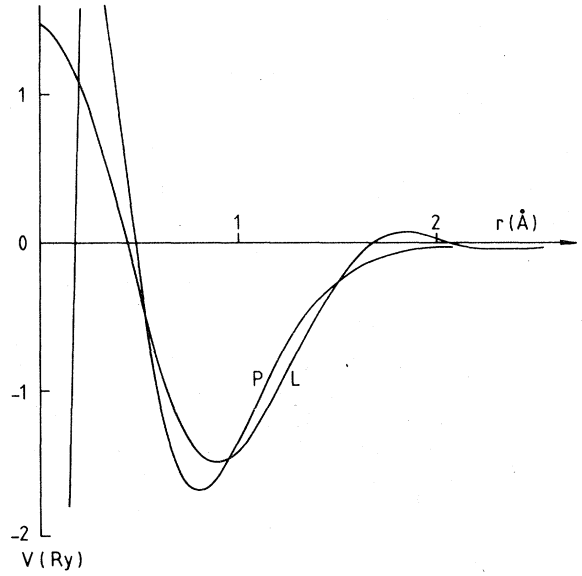


FIG. 1. Average self-consistent vacancy potentials, from Louie (Ref. 9) ($L$) and the present calculation ($P$) described in Sec. III.

tential at small $\vec{k}$ is not important throughout the calculation of bound states because of the dominant role of the short-range interaction. However, $\delta E_T$ cannot be satisfactorily computed without a good appreciation of $V(\vec{r})$ at large $\vec{r}$.

The assessment of $\delta E_T$ is an essential part of our task. In allowing for lattice reconstruction, we have only the change in $\delta E_T$ to guide us as to where the minimum-energy configuration occurs. Fortunately, in the case of a single vacancy in silicon, the formation energy $E_f$ is already known (~5 eV).[31] If we compute the first and second terms in (2.23), $\delta E_{ii}$ can be evaluated to give the experimental $E_f$ and hence the "effective-screening" $\epsilon_f$ at the nearest-neighbor distance. This semiempirical value of the screening constant $\epsilon_f$ can then be used—in the limit of small displacements—in order to find changes in $\delta E_T$ associated with various modes of reconstruction.

## III. NUMERICAL RESULTS

We have carried out a self-consistent pseudopotential calculation concerning the localized states associated with a vacancy in silicon, following the methods outlined in Sec. II. In this section, we will describe our numerical results. An assessment of the work, a comparison with existing theory and experiment, and discussion will be given in Sec. IV.

We first consider the average vacancy potential shown in Fig. 1 ($P$) and apply the Green's-function formalism of Eqs. (2.1) and (2.14) to calculate the bound states in the gap. This calculation is executed in the same manner as those described earlier. We employ a sample of 41 general points in the $\frac{1}{48}$th irreducible segment of the Brillouin zone. The vacancy potential is spherically symmetrical and positioned at the perfect-lattice site from which an atom was removed. The point group of the site is $T_d$ and we recover a threefold-degenerate state in the forbidden gap. The $a_1$ state is approximately 1 eV below the valence-band edge. No attempt was made to locate this state accurately. The position of the $t_2$ state is shown in Fig. 2, as a function of the number of bands included in the expansion (2.2). The effect of scaling upon the position of the bound state in the gap is shown in Fig. 3. Here $s=1$ corresponds to running the program with the potential of Fig. 1($P$).

With our choice of the complete set of functions $g$, the lowest $t_2$ state is exactly "$p$ like" for a spherically symmetrical potential $V$, i.e., the convergence only depends on the number of functions $g$ associated with a spherical harmonic of $l=1$. The best result is shown in Fig. 4.

A sample of 27 points was chosen to represent the volume of the Brillouin zone as uniformly as possible and the linear equations of (2.4) were set up employing the eight lowest bands. The input band structure was derived from the best empirical pseudopotential as was the case in the Green's-function calculation. With the potential of Fig.

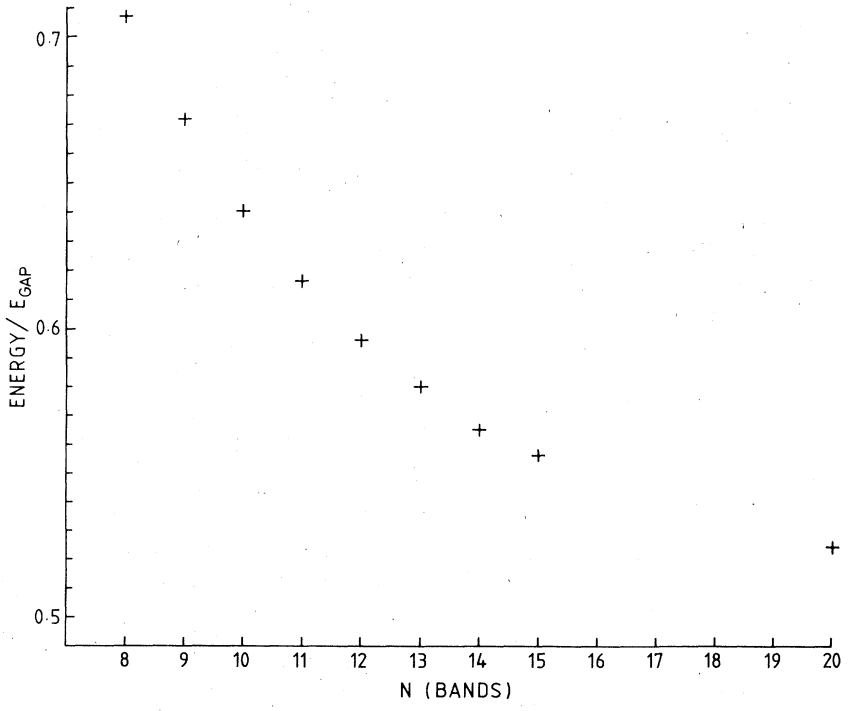


FIG. 2. Energy of the threefold degenerate $T_2$ state in the gap, measured from the top of the valence band of the perfect crystal, as a function of the number of bands included in the expansion of the wave function. All remaining parameters entering the calculation remain unchanged. The method of the calculation is outlined in Sec. II, Eqs. (2.1) and (2.15). The vacancy potential is shown in Fig. 1 ($P$).

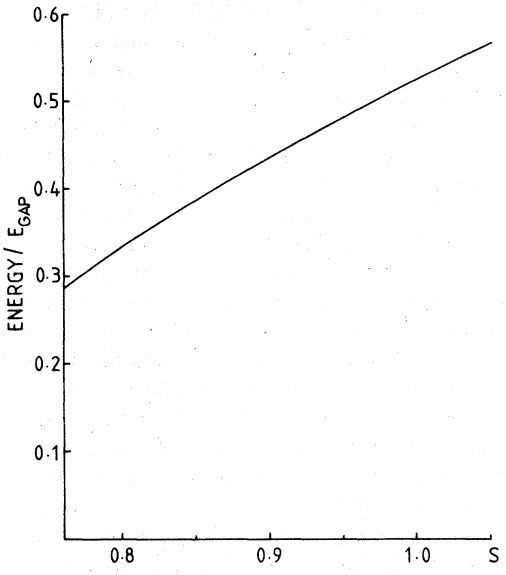


FIG. 3. Effect of scaling the vacancy potential of Fig. 1 ($P$) upon the energy of the $t_2$ state as calculated using the Green's-function method.

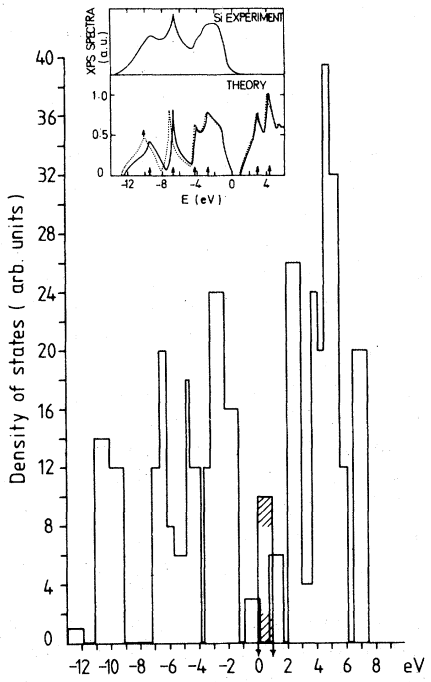


FIG. 5. Perfect-crystal density of states used in the direct-matrix calculation described in Secs. II and III. The full-scale pseudopotential calculations give results shown in the inset (solid line—nonlocal pseudopotential, dotted line—local pseudopotential) from J. R. Chelikowsky and M. L. Cohen, Phys. Rev. B 14, 556 (1976).

1($P$), the threefold-degenerate ($t_2$) state appears at 0.89 $E_9$ above the valence-band edge. The quality of sample used in the calculation is indicated by plotting the density-of-states histogram in Fig. 5. Our tests strongly support the results obtained from studies on similar systems, indicating that the choice of the sample has no—or very little—effect upon the self-consistent procedure of computing the potential $V(\vec{r})$.

The self-consistent potential consists of the bare-model potential $V_b$ of Animalu and Heine,[32,33] represented by an analytic fit,[9] and the potential $V_e$ associated with $\Delta\rho = \rho_{\text{vacancy}} - \rho_{\text{perfect}}$. Through-

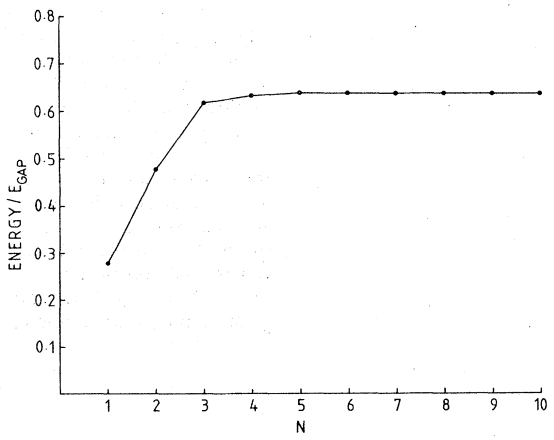


FIG. 4. Bound-state energy as a function of the number of the localized functions $g_m$ (Sec. II). Ten bands were used in Eq. (2.3).

out the calculations it is assumed that only one electron is available to fill the bound states in the gap, i.e., three "dangling electrons" are accounted for. As in the method of Louie *et al.*, the charge "accountancy" is automatically taken care of by correct normalization, incorporated into the computer program which performs the sums over the occupied states via our sampling technique.

The valence charge density, along several directions from the vacancy site, is presented in Figs. 6–9. The curve $A$ corresponds to the perfect-crystal charge-density distribution. The charge density in the presence of the vacancy potential of Fig. 1($P$) is used to construct a new, spherically symmetric potential for $V_{\text{Si}}^{+}$. As expected, this potential was similar to that in Fig. 1($P$). The final charge-density distribution arrived at in this manner is shown in curves $B$, Figs. 6–9. The effect upon the bound state in the gap amounted to bringing the energy down by 0.2 eV. However, it can be seen from our figures that the charge-density distribution is highly anisotropic. In particular, the departure from sphericity is characterized by removing more charge from the bond. We have, therefore, constructed a nonspherical potential which accounts

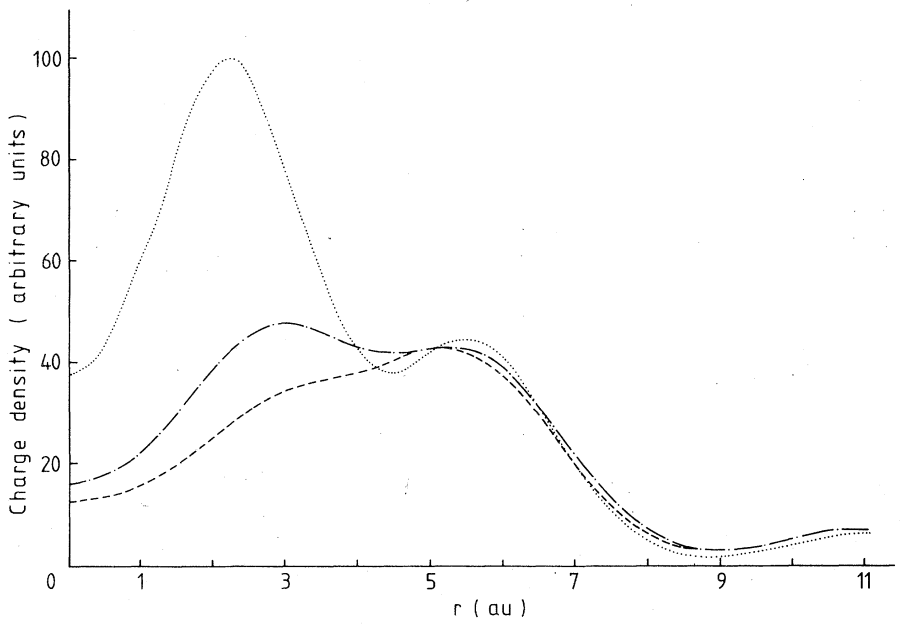


FIG. 6. Valance charge density (excluding that due to the occupied state in the gap), along the ⟨111⟩ direction (towards the nearest-neighbor silicon atom). (*A*) dotted line, perfect crystal; (*B*) dashed line, unreconstructed vacancy (spherical potential); (*C*) dash-dot line, final result corresponding to the minimum-energy configuration (point *A*, Fig. 14).

for the computed charge distribution and which can be fed into our program thanks to the fact that matrix elements are computed in the wave-vector space. The calculation was then allowed to converge to achieve self-consistency and the resulting charge density is shown in Figs. 6–9 (*C*). Although the departure from sphericity represents only a small correction to the *average* vacancy potential, and its impact on the overall valence charge-density distribution is almost negligible, the position of the bound state in the gap is greatly affected and the energy level is reduced to a position 0.21 eV above the valence-band edge. The modulus squared of the wave function associated with the bound state in the gap is plotted in Figs. 10–12. Since the wave function is localized along the "dangling bond" and does not seem to change much with the change in the potential, such a large effect upon the bound-state energy in the gap is only to be expected. We now proceed to find a

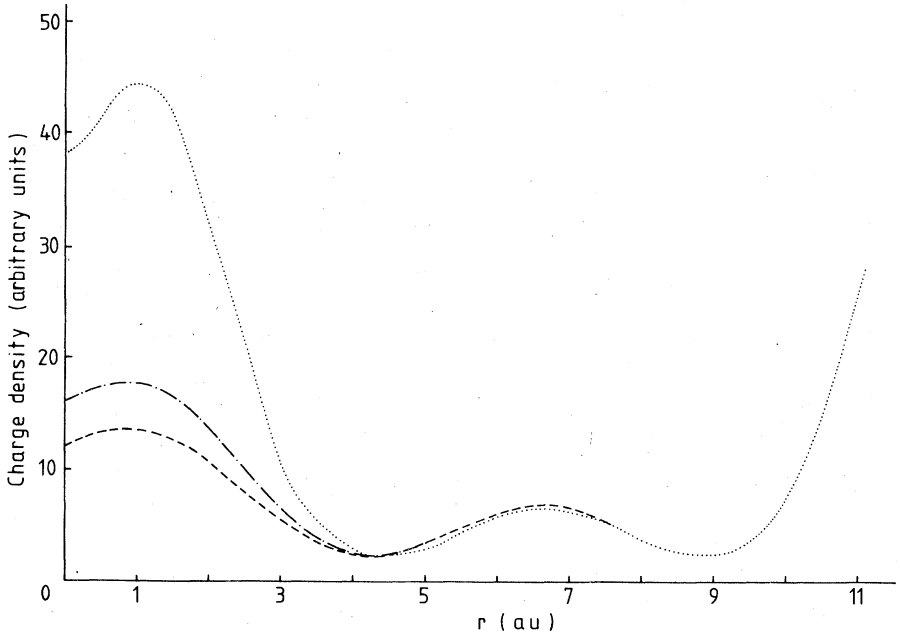


FIG. 7. Valence charge density, along the ⟨111⟩ direction. Notation as in Fig. 6.

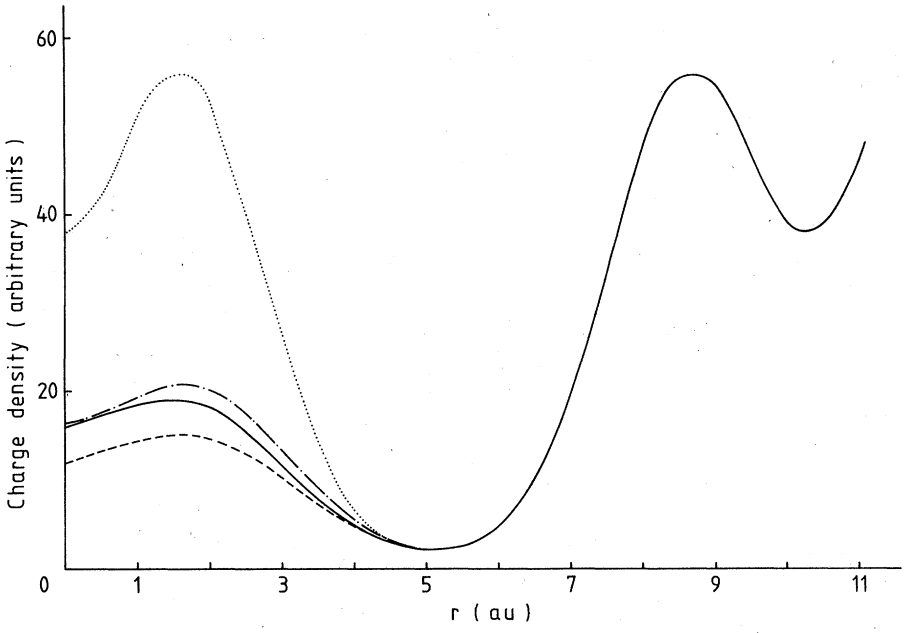


FIG. 8. Valence charge density along the ⟨100⟩ direction. (*A*) dotted line, perfect crystal; (*B*) dashed line, unreconstructed vacancy (spherical potential); (*C*) dash-dot line, unreconstructed vacancy (nonspherical potential); (*D*) solid line, final result corresponding to the minimum-energy configuration (point *A*, Fig. 14).

solution to the vacancy problem in the presence of lattice reconstruction. We will consider three modes of reconstruction, as illustrated in Fig. 13. The group-theoretical analysis shows the effect of an axial field upon the $t_2$ level.[34] We will study in great detail the displacements of the tetragonal type ($D_{2d}$) and "sample" the plane defined by directions 1 and 4, as shown in Fig. 14. The position of the "perfect" ⟨111⟩ direction connecting the vacancy site with that of the nearest-neighbor atom and the experimentally observed axis shifted by 7° towards ⟨100⟩ are also shown. We carry out self-consistent calculations, in exactly the same manner as before, allowing for displacements of the nearest-neighbor atoms along the lines 1, 2, 3, and 4. We plot the final positions of the bound states in the gap in Fig. 15. As expected, in the tetragonal field, the threefold-degenerate state

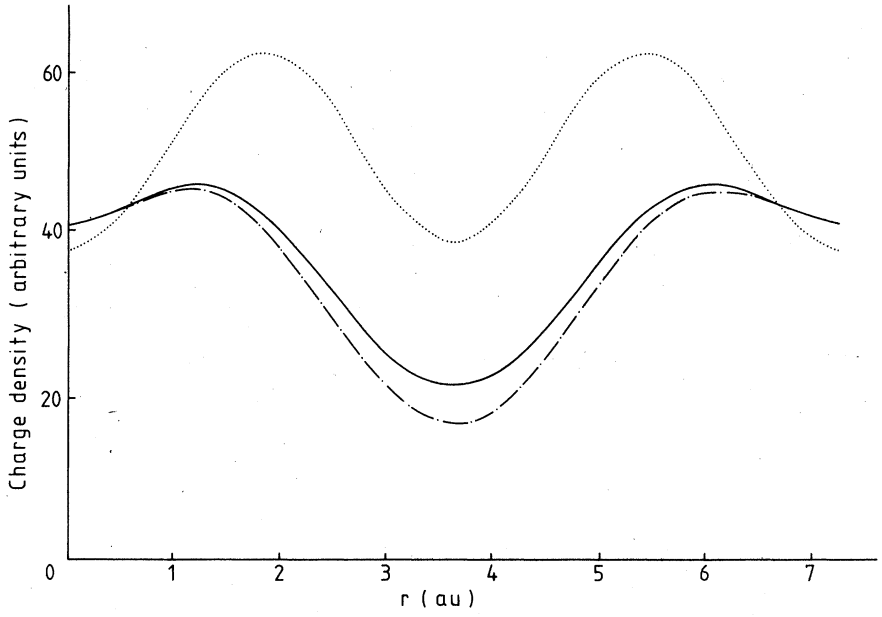


FIG. 9. Valence charge density, along the tetragonal displacement direction connecting two nearest-neighbor silicon atoms. Notation as in Fig. 8.

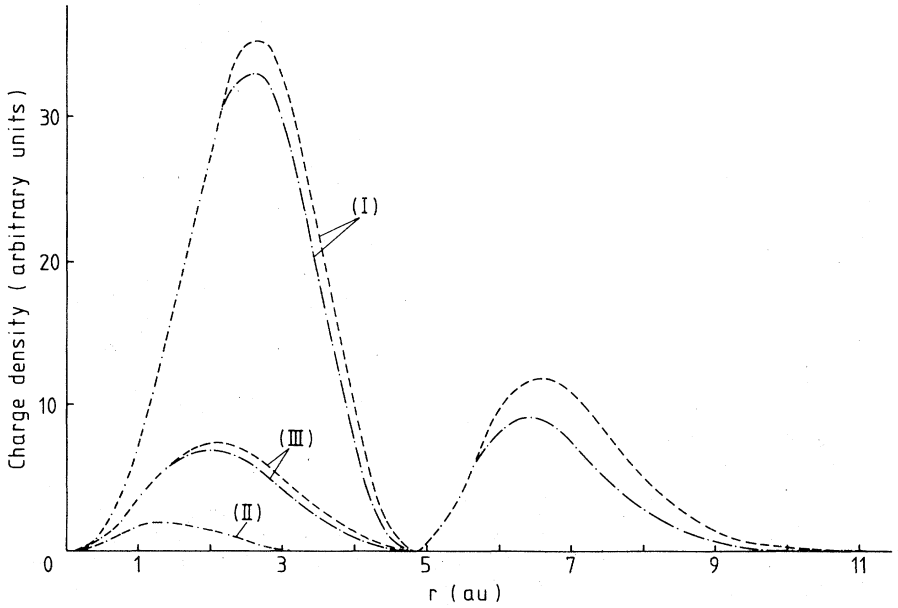


FIG. 10. Charge density associated with the three fold-degenerate localized states in the gap.

I ⟨111⟩ direction
II ⟨$\bar{1}\bar{1}\bar{1}$⟩ direction
III ⟨100⟩ direction

(*A*), (*B*), (*C*), and (*D*) have the same meaning as in Fig. 8. Note the overlap of (*B*) and (*C*) dot–double dash line.

splits into a singlet, marked I, and a two-fold-degenerate state, marked II. The totally symmetric displacements, inward (direction 4) and outward (direction 3), are also shown. We have carried out a less systematic sampling of the other parts of the above-mentioned plane with results confirming the trend shown in Fig. 15. Finally, we compute the change in the total energy of the system, following Eq. (2.23). Since the value of the effective-screening constant $\epsilon_f$ is determined by demanding that the formation energy $E_f$ is close to the experimental value, we choose $E_f = 5$ eV and find $\epsilon_f = 19$, at the perfect-crystal nearest-neighbor distance. The final result, i.e., the change in the total energy along the direction chosen in Fig. 14, is shown in Fig. 16. If the effect of $\delta E_{ii}$ is omitted, the absolute minimum occurs for a symmetric outward displacement, of about 0.17 of the nearest-neighbor distance from the perfect-atom positions.

The trigonal displacement was also considered. We carried out several calculations, displacing the nearest neighbors as indicated in Fig. 13. The results are similar to those obtained for tetragonal

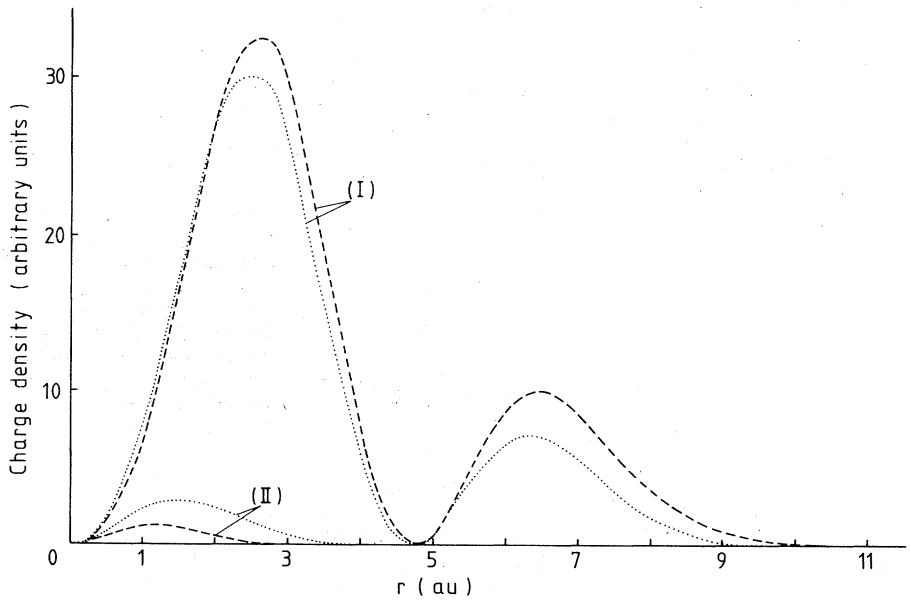


FIG. 11. Final (case *D*) charge distribution associated with the onefold- (dotted line) and twofold- (dashed line) degenerate localized states in the gap, along ⟨111⟩ (curve I) and ⟨$\bar{1}\bar{1}1$⟩ (curve II).

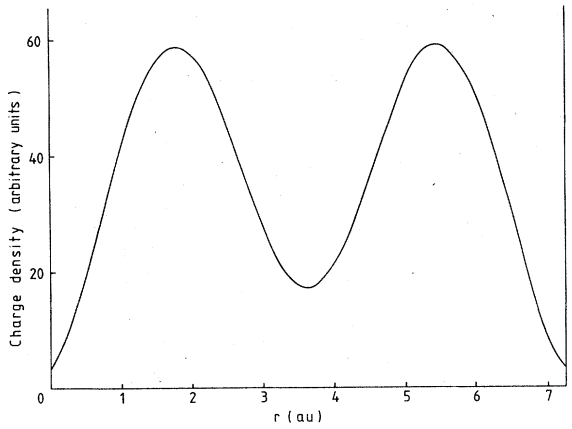


FIG. 12. Charge density associated with the localized state in the gap ($C$) along the line of the tetragonal distortion connecting the nearest-neighbor silicon atoms.

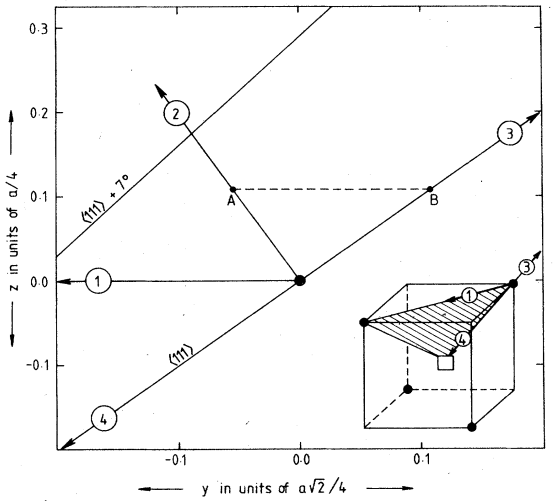


FIG. 14. Plane involving the vacancy and its two nearest neighbors is shown in the inset. The directions 1, 2, 3, and 4 are thus defined, with respect to the perfect-lattice ⟨111⟩ direction. The tilt of 7° is also shown. The positions $A$ and $B$ correspond to the minimum energy ($A$) and minimum gradient ($AB$) points. $a$ is the lattice constant.

displacements. The trigonal field leads to a splitting of the $t_2$ state which is also indicated in Fig. 13. The gain in the total energy appears to be smaller than that shown in Fig. 16. However, a systematic examination of the trends was not performed.

## IV. DISCUSSION

It is not the prime purpose of this calculation to establish precise positions of the bound states in the forbidden gap. Neither the accuracy of the input ("local"-model potentials) nor the precision with which we are prepared to execute our calculations seem adequate for such a task. However, we must ensure that the most important terms in the Hamiltonian have been correctly accounted for so that the overall features yielded by the numerical experiment bear comparison with reality. For it is the aim of this calculation to reveal the nature of physical processes underlying the formation of localized states. Strictly speaking, we wish to capture the "signature" of the defect. One of the most important factors here is the symmetry of the system under consideration. In particular, we would like to understand the magnitude of the ef-

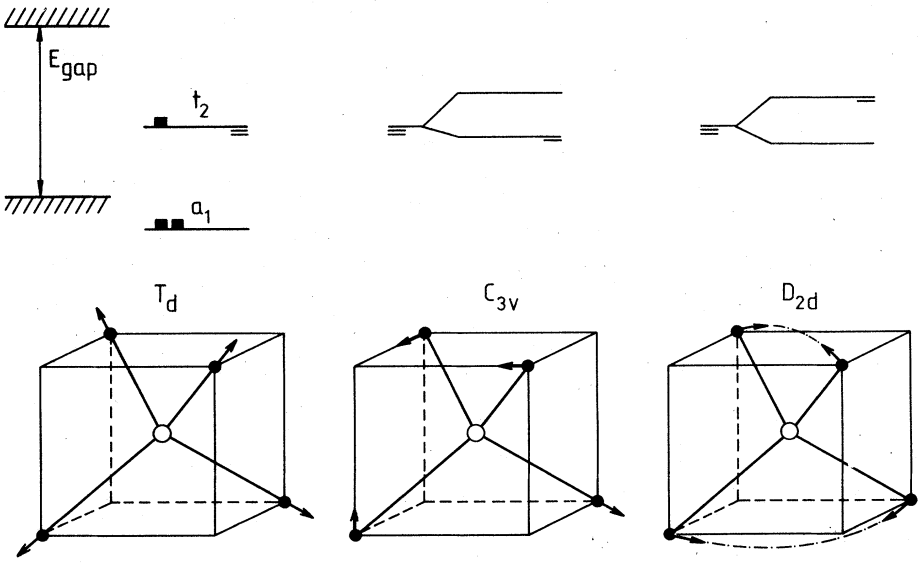


FIG. 13. Tetrahedral ($T_d$), trigonal ($C_{3v}$), and tetragonal ($D_{2d}$) configurations of the nearest-neighbor silicon atoms are indicated. The localized levels associated with the vacancy in a given environment are indicated schematically.

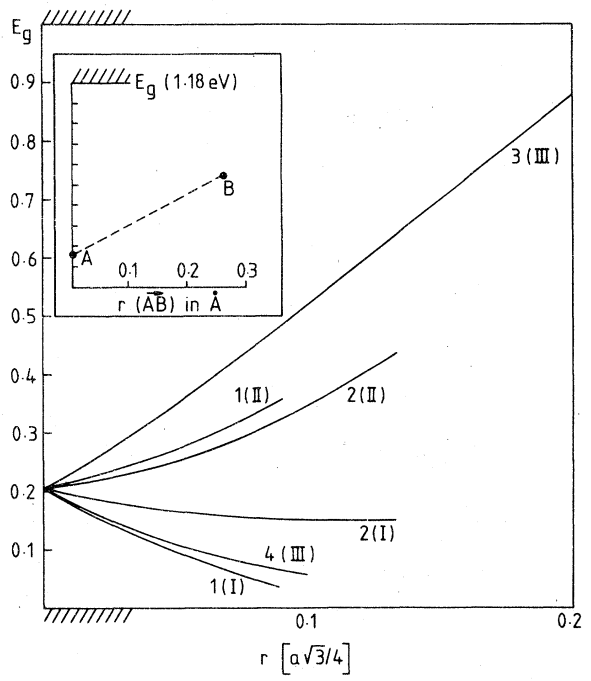


FIG. 15. Effect of the distortions 1–4 defined in Fig. 14 upon the localized levels in the forbidden band gap. I, II, and III refer to the onefold-, twofold-, and threefold-degenerate states, respectively. The displacements are measured in the units of the perfect-crystal nearest-neighbor distance, $\frac{1}{4}a\sqrt{3}$. The behavior of the lowest state along the path $AB$ is shown in the inset. The $r=0$ point refers to the self-consistent solution before reconstruction. The results are discussed in Secs. III and IV.

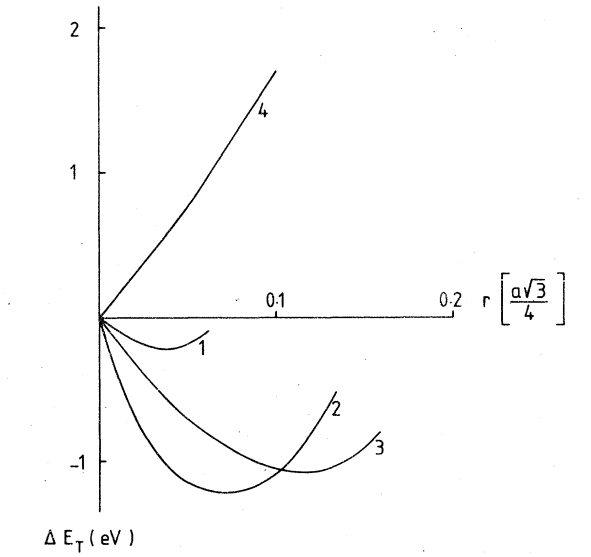


FIG. 16. Change in the total energy $\Delta E_T$ of the system containing a positively charged vacancy ($V_{Si}^{+}$), for displacements defined in Fig. 14.

fect of lattice distortion and formulate the relevant questions in quantitative terms.

### A. Localized states

Both the Green's-function and direct-matrix calculations indicate a $t_2$ state in the lower part of the gap. In this study, no effort will be made to narrow the errors by using Eqs. (2.17) and (2.19) so that the position could be identified accurately. It transpired that the overall characteristics of the defect, i.e., the localization and form of the wave function as well as the effect of lattice distortion, are insensitive to such details. Although our computer power is far from being exhausted by the demands posed by overall convergence requirements, there is very little hope of finally settling this matter at the present stage. This is well demonstrated by the effect of introducing nonspherical potentials. Although there is a systematic shift between the absolute positions of the levels predicted by the Green's-function and direct-matrix methods, both schemes show in very much the same way that the position of the level in the gap is sensitive to the changes in the nonspherical part of the vacancy potential. This term is very difficult to compute with precision because it represents only a small part of the total potential and suffers most from inadequacies in the numerical procedures. As we have mentioned earlier, the nonspherical part of the potential is related to the changes in the charge density localized on the bond between the vacancy and its nearest neighbors. It is borne in mind that differences in predicted *absolute* positions of the levels in the gap between self-consistent calculations of similar convergence properties may be largely due to differences in technical details of handling the nonspherical part of the potential. We have carried out a number of calculations designed to test whether this ambiguous element has any effect upon the *overall picture* emerging from Figs. 14–16. This pattern of the splittings, and their relationship to the form of reconstruction, is remarkably *insensitive* not only to the strength of the average potential but also to the method of handling the angular forces. However, we are aware that the task of accurately locating bound states with respect to the band edges is of general importance since it enables us to assess the electrical properties of the materials. In particular, it is of interest to characterize the various charge states of the defect. We will present a detailed study of the position of localized states in a separate publication.

### B. Minimum-energy configuration

We have noted a most surprising insensitivity of our predictions of the form of lattice reconstruction to the details of the potential and also, for that matter, to any other details of the calculation. The change in the band-structure contribution to the change in the total energy, $\delta E_T - \delta E_{ii}$, always favors an outward symmetric displacement. Although the magnitude of the displacement does vary depending on the form and strength of the potential, the predicted change in the position of the nearest-neighbor atoms appears around 10%–15% of the nearest-neighbor distance in all cases. The effect of $\delta E_{ii}$ favors inward displacements and does alter the position of the minimum-energy point.

As we can observe in Fig. 16, the difference in the energy minima identified along directions 2 and 3 is very small. On the other hand, the path with a very small energy gradient, indicated in the inset of Fig. 15 (see also points $A$ and $B$ in Fig. 14), corresponds to a very marked change in the position of the bound state. Unfortunately, the actual position of the absolute minimum shown in Figs. 14–16 cannot be taken too seriously because it depends critically upon the semiempirical factor $1/\epsilon_f$ and the absolute magnitude of $\delta E_{ii}$.

The formation energy $E_f$ is one of the most important characteristics associated with defects like vacancies. As we remarked earlier, all three terms in Eq. (2.23) are of the same order of magnitude, i.e., ~10 eV and $\delta E_T$ is the result of competition between these terms. The experimental data for formation energies of single vacancies in diamond-type semiconductors indicate[31] $E_f(V_{\mathrm{Si}})$ ~4–5 eV, $E_f(V_{\mathrm{Ge}})$ ~ 2–3 eV. It is difficult to see how we could achieve an accuracy of 0.1 eV in determining $E_f$, i.e., the accuracy which would enable us to compare the results for silicon with those for germanium. On the other hand, our preliminary calculations on other types of defects, e.g., interstitials, show that the *differences* in $E_f$ are larger than 1 eV. The calculations carried out on defects in diamond[35-37] seem to point in the same direction. It seems that comparisons of $E_f$'s for sufficiently different defects in a given material, i.e., their assessment on a relative scale in, say, silicon, should be possible with our present means.

### C. Comparison with the existing theoretical and experimental evidence concerning the vacancy in silicon

It is instructive to visualize the defect in a simpler way, derived from the defect-molecule model.[38] We remove the central atom and keep the electronic structure of the rest of the lattice without alterations. The dangling electrons should occupy the $t_2$ and $a_1$ localized states. As expected, all existing calculations predict the symmetric $a_1$ state to occur deep in the valence band. Hence, the remaining dangling electrons occupy the $t_2$ state. With only one electron in the $t_2$ state, we are left with the $V_{\mathrm{Si}}^{+}$ charge state, with two we have the neutral state $V_{\mathrm{Si}}^{0}$, etc. The $t_2$ state is localized on the nearest-neighbor atom. If we now allow for both electronic and lattice relaxation, the threefold-degenerate $t_2$ state may undergo a Jahn-Teller splitting. The $V_{\mathrm{Si}}^{+}$ state is paramagnetic and the ESR results indicate that the electrical level position is close to the valence-band edge. The analysis[10-14] of the ESR signal reveals that about 66% of the corresponding wave function is localized on the four nearest neighbors. The $Si^{29}$ hyperfine interactions indicate a tetragonal distortion involving a tilt of 7.2° from the perfect ⟨111⟩ direction toward ⟨100⟩. The application of external stress changes the energy of the level and it was estimated that the level rises at a rate $\Gamma = 2.9$ eV/Å.

It is worth mentioning that the parameter $\Gamma$ is deduced from the experimentally determined change in the energy of defect reorientation $\Delta E_i$ by assuming $\Delta E_i = \Gamma Q$, where $Q$ is the amplitude of the lattice displacement of the particular mode under stress. Since it is difficult to know $Q$ in the distorted lattice, the coefficient $\Gamma$ seems rather uncertain. However, the results outlined above do offer a sufficiently clear picture and many attempts have been made to explain it. It is not our intention to review the numerous contributions made by a number of authors during the last decade. However, we note that for an unrelaxed vacancy all existing calculations yield an $s$-like state in the valence band and a $p$-like ($t_2$) state in the forbidden gap. Because of the formidable convergence problems discussed in Secs. I–III, it seems futile—at least at this stage of development—to enter a detailed argument concerning the assessment of the methods on the strength of their prediction of $E_{t_2}$. If we estimate the position of the $t_2$ state, combining our results obtained from the Green's-function and direct-matrix methods, we arrive at $E_{t_2}(V_{\mathrm{Si}}^{+}) = E_v \pm 0.2$ eV, where $E_v$ is the energy at the top of the valence band. Both the uncertainty in the convergence in bands and our inability to handle unambiguously the nonspherical potential are significant sources of error. These problems are not peculiar to our method, although they may take on a different numerical form depending on the scheme employed. Certainly, the pseudopotential band structure above, say, the tenth band, becomes quite unreliable and because of the many-fold nature of the convergence pro-

cess (bands, points, plane waves, and the potential), it is doubtful whether the slow convergence seen in Fig. 2 is "real." As for the potential, there can be no unique way of separating a nonspherical potential into mathematically treatable units. Therefore, the most important aim of any calculation concerning the vacancy is to establish the form of the lattice distortion. This has been attempted in a few earlier calculations. Larkins carried out a number of computations and gave a thorough account of his efforts. Unfortunately, the symmetric relaxation predicted was so large that it made the vacancy formation energy negative.[4,39,40] The calculations of Yip[41] predict an outward relaxation of about 13% of the nearest-neighbor distance, in accord with the work of Messmer and Watkins on diamond.[2] Since they did not include the effect of ion-ion interaction in their assessment of the final configuration, their prediction is in line with our results described in Sec. III. Messmer and Watkins[2] pointed out that much of the observed tilt in the hyperfine spectra may not be due to Jahn-Teller distortion but merely a result of the proximity of the localized state to the valence band. Our results suggest that the precise position of atoms depends very much on the magnitude of $\delta E_{ii}$.

We have remarked in Sec. III on the nature of the splitting of the $t_2$ state under the influence of axial fields. Previous calculations revealed that this splitting is small and relatively insensitive to the details of the potential. This is well supported by our results although it must be observed that the splitting *is* sensitive to the mode of atomic displacement (Fig. 15). Unfortunately, no direct evidence is available as far as the splitting is concerned since the stress experiments merely indicate the change in the position of the ground state with respect to the valence band. If, as a result of the application of stress, the nearest-neighbor atoms moved from their minimum energy at position $A$, Fig. 15, along the line indicating the lowest energy gradient, then the level in the gap rises at a rate of ~2 eV/Å (Fig. 15). This compares well with the rate quoted by Watkins—2.9 eV/Å—considering the uncertainties involved.

The traditional approach to the determination of the electronic structure of defects and their energy levels in the forbidden gap is based on the one-electron theory. It begins with the one-electron eigenstates of the perfect-crystal Hamiltonian and attempts to construct the self-consistent description of the system in terms of a linear combination of these functions. The cluster approach is normally based on some form of one-electron molecular-orbital method. The assumption has been made that many-electron effects are small and can be ignored. In the case of a vacancy in a diamond-type semiconductor, such a simplification may be challenged since several highly localized particles are likely to be involved. Indeed, Coulson and Larkins[42] concluded that no substantial reduction in the many-electron effects should take place as a result of delocalization of the atomic states when immersed into a solid. However, the calculations of Watkins and Messmer,[37] based on the self-consistent-field $\chi\alpha$ scattered-wave method of Johnson, Slater, and Smith,[43] do indicate that as the cluster becomes more representative of a solid, the delocalization of the eigenstates reduces the many-electron effects. Although it remains uncertain to what extent this result can be regarded as final and of general validity, it does provide the much needed support to the one-electron theory.

## V. SUMMARY AND CONCLUSIONS

We have performed a self-consistent pseudopotential calculation of the electronic states of a single vacancy in silicon. The bound states were studied using both the Green's-function formulation and the direct-matrix method. The latter also yields the valence charge density and enables us to carry out the calculation of the change in the total energy of the system.

We argue that the convergence properties of the bound-state calculation are different from those of the calculation of the sums over electron energies and wave functions involving the valence-band states in the presence of the defect. We propose that it is reasonable to exploit the technical relationships by splitting the computational procedure into several stages and tailoring the methods of dealing with them so as to allow for the most tractable solution of the problem. To position a bound state with an accuracy adequate for a quantitative comparison with experiment. e.g., ±50 meV on an absolute scale, still seems to be an impossible task. We have seen, in this and other calculations, that the energy of the level measured from the relevant band edge is a small number resulting from a cancellation process of large contributions. Both the "bare" and the electron potentials contain errors which are difficult to quantify. Probably this is not where the most fruitful contact with experiment should be expected, although scope still remains for more exhaustive computational endeavors. Technically, the most ambiguous aspect of the computational process lies in the fact that the potential fed into the calculation is not spherically symmetric. However, the relative changes in the binding energy which only involve corrections to the bulk of the localized

potential should be much easier to calculate. The changes in the valence charge density due to the effects of the defect potential and lattice reconstruction vary smoothly and do not appear to be very sensitive to the details of the procedure employed. All results are sensitive to the symmetry of the lattice reconstruction, although the actual displacements of atoms are within ~0.1 Å. The most serious obstacle in the path of our efforts to compute changes in the total energy of the system is our inability to estimate the long-range properties of the localized potentials.

We found that the positively charged vacancy has a localized state at the valence-band edge. The lattice reconstruction consists of a symmetric (outward) displacement of the nearest-neighbor atoms and a tetragonal displacement whose precise magnitude is difficult to establish. The total displacement is about 0.1–0.2 Å. The net reduction in the total energy associated with the lattice reconstruction is about 1 eV.


[1]W. Kohn, in *Solid State Physics*, edited by F. Seitz and D. Turnbull (Academic, New York, 1957), Vol. 5, p. 257.
[2]R. P. Messmer and G. D. Watkins, Phys. Rev. B 7, 2568 (1973).
[3]L. A. Hemstreet, Phys. Rev. B 15, 834 (1977).
[4]F. P. Larkins, J. Phys. Chem. Solids 32, 965; 2123 (1971).
[5]M. Jaros, J. Phys. C 8, 2455 (1975).
[6]M. Jaros and S. Brand, Phys. Rev. B 14, 4494 (1976).
[7]J. Bernholc and S. T. Pantelides, Phys. Rev. B 18, 1780 (1978).
[8]S. T. Pantelides, Rev. Mod. Phys. (to be published).
[9]S. G. Louie, M. Schlüter, J. R. Chelikowsky, and M. L. Cohen, Phys. Rev. B 13, 1654 (1976).
[10]G. D. Watkins, J. Phys. Soc. Jpn. 18, 22 (1963).
[11]G. D. Watkins, in *Radiation Damage in Semiconductors* (Dunod, Paris, 1964), p. 97.
[12]E. L. Elkins and G. D. Watkins, Phys. Rev. 174, 881 (1968).
[13]G. D. Watkins, in *Radiation Effects on Semiconductor Components I* (Journees d'Electronique, Toulouse, 1967), p. A1.
[14]G. D. Watkins, in *Radiation Damage and Defects in Semiconductors*, edited by J. E. Whitehouse (Institute of Physics, London, 1973), p. 228.
[15]L. C. Kimerling, in *Radiation Effects in Semiconductors*, edited by N. B. Urli and V. W. Corbett (Institute of Physics, London, 1976), p. 221.
[16]F. Bassani, G. Iadonisi and B. Preziosi, Phys. Rev. 186, 735 (1969).
[17]S. Brand, J. Phys. C 11, 4963 (1978).
[18]G. F. Koster and J. C. Slater, Phys. Rev. 95, 1167 (1954); 96, 1208 (1954).
[19]J. Callaway and A. J. Hughes, Phys. Rev. 156, 860 (1967).
[20]R. A. Faulkner, Phys. Rev. 175, 991 (1968).
[21]M. Jaros, Phys. Rev. B 16, 3694 (1977).
[22]M. L. Cohen and V. Heine, in *Solid State Physics*, edited by H. Ehrenreich, F. Seitz, and D. Turnbull (Academic, New York, 1970), Vol. 24, p. 37; V. Heine and D. Weaire, *ibid.*, p. 249.
[23]L. J. Sham and J. M. Ziman, in *Solid State Physics*, edited by F. Seitz and D. Turnbull (Academic, New York, 1963), Vol. 15, p. 221.
[24]P. K. W. Vinsome and M. Jaros, J. Phys. C 3, 2140 (1970).
[25]P. K. W. Vinsome and D. Richardson, J. Phys. C 4, 2650 (1971).
[26]J. P. Walter and M. L. Cohen, Phys. Rev. 32, 1821 (1970).
[27]J. A. Appelbaum and D. R. Hamann, Phys. Rev. Lett. 32, 225 (1974).
[28]M. Schlüter, J. R. Chelikowsky, S. G. Louie, and M. L. Cohen, Phys. Rev. Lett. 34, 1385 (1975).
[29]M. Schlüter, J. R. Chelikowsky, S. G. Louie, and M. L. Cohen, Phys. Rev. B 12, 4200 (1975).
[30]M. Jaros and S. F. Ross, in *Physics of Semiconductors*, edited by M. H. Pilkuhn (Teubner, Stuttgart, 1974), p. 401.
[31]A. B. Lidiard, Sci. Prog. (London) 56, 103 (1968).
[32]I. V. Abarenkov and V. Heine, Philos. Mag. 12, 529 (1965).
[33]A. O. E. Animalu and V. Heine, Philos. Mag. 12, 1249 (1965).
[34]M. D. Sturge, in *Solid State Physics*, edited by F. Seitz and D. Turnbull (Academic, New York, 1967), Vol. 20, p. 92.
[35]S. P. Singhal, Phys. Rev. B 4, 2497 (1971).
[36]C. Wigel, D. Peak, J. C. Corbett, G. D. Watkins, and R. P. Messmer, Phys. Rev. B 8, 2906 (1973).
[37]G. D. Watkins and R. P. Messmer, Phys. Rev. Lett. 32, 1244 (1974).
[38]C. A. Coulson and M. J. Kearsley, Proc. R. Soc. A 241, 433 (1957).
[39]F. P. Larkins and A. M. Stoneham, J. Phys. C 4, 143 (1971).
[40]F. P. Larkins, J. Phys. C 4, 3065 (1971); 4, 3077 (1971).
[41]K. L. Yip, Phys. Status Solidi B 66, 619 (1974); K. L. Yip and W. B. Fowler, Phys. Rev. B 10, 1400 (1974).
[42]C. A. Coulson and F. P. Larkins, J. Phys. Chem. Solids 32, 2245 (1971).
[43]K. H. Johnson and F. C. Smith, Jr., Phys. Rev. B 5, 831 (1972); J. C. Slater and K. H. Johnson, Phys. Rev. B 5, 844 (1972).